chemistry

Article

Long-Range Supramolecular Synthon Isomerism: Insight from a Case Study of Vinylic Tellurium Trihalides Cl(Ph)C=C(Ph)TeX_3 (X = Cl, I)

Yury V. Torubaev [1,*] and Aida S. Samigullina [2]

1 N.S. Kurnakov Institute of General and Inorganic Chemistry, Russian Academy of Sciences, 119991 Moscow, Russia
2 N.D. Zelinsky Institute of Organic Chemistry, Russian Academy of Sciences, 119991 Moscow, Russia; s_aida_88@mail.ru
* Correspondence: torubaev@igic.ras.ru

Abstract: A slight modification of the synthetic procedure resulted in a new (*Cc*) polymorph of vinylic tellurium-trichloride Z-Cl(Ph)C=C(Ph)$TeCl_3$ (**1,** β-form) which is stabilized by Te· · · Cl chalcogen bonds, assembling its molecules into the zigzag chains. Such a packing motive is in contrast to the known ($Pca2_1$) polymorph of Z-Cl(Ph)C=C(Ph)$TeCl_3$ (**1,** α-form, CCDC refcode: BESHOW), which is built upon Te· · · π(Ph) chalcogen bonded chains. We noted a similar case of [Te· · · halogen] vs. [Te· · · π(Ph)] supramolecular synthon polymorphism in its triiodide congener Z-Cl(Ph)C=CPh(TeI_3) (**2,** α and β-polymorphic forms). Quantum chemical calculations of the intermolecular interaction and lattice energies for **1**α–β and **2**α–β supported the assumption that α is thermodynamic while β is a kinetic form. Kinetic forms **1**β and **2**β are isostructural (*Cc*), while the thermodynamic forms **1**α ($Pca2_1$) and **2**α ($P2_1/c$) are not and feature an unusual example of *long-range supramolecular synthon module isomerism*. In other words, **1**α–**2**α pairs demonstrate very similarly to isostructural Te· · · πPh ChB stabilized chains, which are further packed differently relative to each other, following different angular geometry of type-I Cl· · · Cl and type-II I· · · I halogen bonding. These structural considerations are backed by quantum chemical calculations that support the proposed hierarchy of primary and secondary supramolecular synthons and the assignment of α and β as thermodynamic and kinetic forms, respectively.

Keywords: chalcogen bonding; polymorphism; disappearing polymorph; organotellurium; supramolecular synthon; LSAM; synthon module; noncovalent interactions

check for updates

Citation: Torubaev, Y.V.; Samigullina, A.S. Long-Range Supramolecular Synthon Isomerism: Insight from a Case Study of Vinylic Tellurium Trihalides Cl(Ph)C=C(Ph)TeX_3 (X = Cl, I). *Chemistry* **2022**, *4*, 196–205. https://doi.org/10.3390/chemistry4010017

Academic Editors: Damiano Tanini and Michael D. Ward

Received: 2 January 2022
Accepted: 15 March 2022
Published: 17 March 2022

1. Introduction

A growing interest in halogen bonding (HaB) [1] and other σ-hole interactions [2,3] in the past two decades has provided a more profound understanding of chemical bonding and enriched the inventory and scope of crystal engineering [4–8]. In most case, these specific and directional interactions can be considered as the extended case of hypervalent 3c–4e interactions, allowing the consideration of intermolecular interactions in terms of molecular orbitals. This is particularly true and important for the heavy main group p-elements so that the structural chemistry of, say, organotellurides is extremely rich owing to the pervasive tendency of Te for the specific intermolecular interactions spanning the 3c–4e (hypervalent) and chalcogen bonding [9–11]. Attractive intermolecular interactions between the electrophilic atoms of Te and nucleophilic halogens (or other HaB-acceptors) are examples of chalcogen bonding (ChB, "a sister of halogen bond" [12]) and are so frequent in the solid state that their absence is sometimes more notable than their presence [13].

Recently, we have investigated the interaction of ferrocene with Ph_2C_2(Cl)$TeCl_3$ and described a series of ferrocenium cocrystalline salts with partly hydrolyzed Ph_2C_2(Cl)$TeCl_3$ [14]. We were quite surprised to notice that characteristic Te· · · Cl intermolecular interactions are absent in the crystal structure of $Ph_2C_2(Cl)TeCl_3$ as reported earlier [14] (**1**, hereinafter referred to as the **α**-form), so that only the Te$\cdots\pi$Ph-specific packing motif or supramolecular synthon (further abbreviated as SS) can be found in it. Later, during the routine PXRD analysis of $Ph_2C_2(Cl)TeCl_3$ sample synthesized for this project by a slightly modified procedure, we found (and were quite surprised once again) that we have a new polymorph of $Ph_2C_2(Cl)TeCl_3$ on our hands (hereinafter referred as the **1β**), which, according to the SC-XRD analysis, features the anticipated Te$\cdots$Cl SS instead of Te$\cdots\pi$Ph. This suggested the preparation of triiodide congeners $Ph_2C_2(Cl)TeI_3$ and a closer comparative examination of the polymorphism and peculiarities of the crystal structure in this series.

2. Materials and Methods

All reactions and manipulations were performed using the standard Schlenk techniques under an inert atmosphere of pure nitrogen or argon. Solvents and SO_2Cl_2 were purified, dried and distilled in argon atmosphere before use. Commercial reagents (Ph_2C_2, Te, KI) were used without additional purification. $TeCl_4$ was prepared according to the procedure reported by Petragnani et al. [15].

*2.1. Preparation of Trichloro (Z)-2-Chloro-l,2-diphenylvinyl-tellurium(IV) Z-Cl(Ph)C=C(Ph)TeCl$_3$ (**1α** and **1β**)*

Powdered Te (1.37 g, 10 mmol) was refluxed with neat SO_2Cl_2 (10 mL, excess) for 3 h. After washing the solid residue with dried hexanes, as described in the original procedure for the preparation of $TeCl_4$ [16], the whole portion of crude $TeCl_4$ was refluxed with Ph_2C_2 (1.9 g, 10 mmol) in CCl_4 (5 mL) for 2 h. Further slow cooling of the reaction mixture afforded a yellow crystalline conglomerate, which was crushed and washed with cold hexane (3 × 10 mL), then dried in vacuum. It consisted of the crystals suitable for a single crystal and powder XRD analysis and was defined as a new (**β** polymorph) form of Z-Cl(Ph)C=C(Ph)$TeCl_3$ (**1β**). Crude **1β** resulted in **1α** upon recrystallization from hot CCl_4.

*2.2. Preparation of Triiodo [(Z)-2-Chloro-l,2-diphenylvinyl-tellurium(IV) Cl(Ph)C=C(Ph)TeI$_3$ (**2**)*

The light yellow solution of **1β** (0.45 g, 1 mmol) in 5 mL of acetone was stirred with powdered KI (1.7 g, 10 mmol) for 12 h. The resulting dark red reaction mixture was dried in a vacuum, washed with hexane and extracted with CH_2Cl_2 (5 × 3 mL). The dark red extract was concentrated with hexane (3 mL) to 1/4 of the initial volume and kept at 4 °C for 12 h. Dark red crystalline precipitate was separated, washed with cold hexane, dried in a vacuum and used for single crystal X-ray investigation. The sample was defined as the isomorphic to **1β** polymorphic form of Z-Cl(Ph)C=C(Ph)TeI_3 (hereinafter referred to as **2β**). Further concentration and cooling of the mother liquor produced an additional quantity of dark red crystalline precipitate of **2β**.

Recrystallization of **2β** from a diluted CH_2Cl_2/hexane (1:3) solution, as well as slow vapour diffusion of pentane into its solution in CH_2Cl_2 at 4 °C, afforded dark red crystals of a new polymorph of **2**, featuring structural resemblance with **1α** (hereinafter referred as **2α**).

2.3. X-ray Crystallography

2.3.1. Single-Crystal XRD

Suitable X-ray quality crystals of **1–2** were obtained directly during the preparation or recrystallization procedures (see preparation details). A Bruker SMART APEXII diffractometer equipped with a graphite-monochromated Mo Kα radiation (0.71070 Å) was used for cell determination and intensity data collection for the cocrystals **1–2**. The data were collected by the standard phi–omega scan techniques and were reduced using SAINT v8.37A (Bruker, Billerica, MA, USA, 2015). The SADABS (Bruker, 2016) software was used for scaling and absorption correction. The structures were solved by direct methods and refined by full-matrix least-squares against F^2 using Olex2 and SHELXTL software (Bruker, Madison, WI, USA) [17,18]. Non-hydrogen atoms were refined with anisotropic thermal parameters. All hydrogen atoms were geometrically fixed and refined using a riding model. Atomic coordinates and other structural parameters of the reported cocrystals have been deposited at the Cambridge Crystallographic Data Center CCDC 2125950 (**1β**), CCDC 2125951 (**2α**) and CCDC 2125949 (**2β**) contains the supplementary crystallographic data for this paper.

2.3.2. PXRD

Powder XRD patterns were obtained at ambient conditions on a Bruker D8 Advance automatic X-ray diffractometer equipped with a Vario attachment and a Vantec linear coordinate detector (CuKα1 radiation, λ = 1.54063 Å, a curved Johansson monochromator; the X-ray tube mode was 40 kV and 40 mA). The samples were ground and deposited onto a silicon plate without strong pressing. The diffraction patterns were recorded in the Bragg–Brentano geometry for 2θ ranges of 5–90° or 5–60° with a step size of 0.008° and 1 or 4 s per step collection time. The samples were rotated in their planes at a rate of 15 rpm to eliminate the influence of preferred orientation and average data. The PXRD diffraction data were processed using the EVA program package (Bruker AXS, 2005) and Bruker TOPAS 5 software [19]. For the calculation of theoretical diffraction patterns, the data from X-ray single-crystal experiments were used. Crystallographic data for 1α were taken from the CSD (refcod BESHOW).

2.4. Intermolecular Energy Computations

Total pairwise energies of interactions between molecules for **1–2α** and **1–2β** and subsequent energy framework [20] generation was performed in Crystal Explorer 21.5 (TONTO, B3LYP-DGDZVP) Crystal Explorer [21] for all unique molecular pairs in the first coordination sphere of a molecule (5 Å) using experimental crystal geometries. The lattice energy of **1–2α**, **1–2β** was estimated as the sum of all unique bimolecular interactions for each independent molecule in the 25 Å coordination sphere [22].

3. Results and Discussion

*3.1. Preparation and Crystal Structure of New Polymorph of Ph(Cl)C=C(Ph)TeCl3 (**1β**)*

Modification of the reported preparation of Cl(Ph)C=C(Ph)$TeCl_3$ [16] by reducing the quantity of the solvent (CCl_4) produced a solid agglomerate of quite well-formed crystals of Cl(Ph)C=CPh($TeCl_3$) (**1β**, *Cc*) after cooling of the refluxed reaction mixture down to room temperature. Such a condition, usually considered to favour the formation of kinetic crystals, allowed the new polymorph, featuring the 1D catemer chains assembled by Te···Cl ChBs (3.449(2)Å, Figure 1b), in addition to the known, presumably thermodynamic polymorph (**1α,** *Pca*2_1, BESHOW [16])), which has Te···π(Ph) chalcogen bonded chains (Figure 1a).

3.2. Preparation and Crystal Structure of Ph(Cl)C=C(Ph)TeI_3

Tellurium tetrachloride ($TeCl_4$) is the only tellurium tetrahalide which is sufficiently reactive for addition to the C≡C triple bond of Ph_2C_2, affording Z-Cl(Ph)C=C(Ph)$TeCl_3$ (**1**). We have prepared corresponding triiodide Z-Cl(Ph)C=C(Ph)TeI_3 (**2**) by treatment with acetone solution of **1** with powdered KI at room temperature (Figure 2).

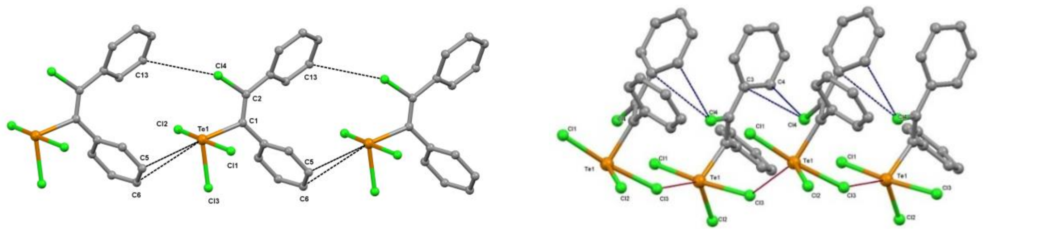

(**a**) (**b**)

Figure 1. Packing pattern of *Z*-Cl(Ph)C=C(Ph)$TeCl_3$ molecules in the polymorphic forms **1α** (*Pca*2_1, refcode BESHOW [14]) (**a**) and **1β** (Cc) (**b**). Hydrogen atoms are omitted for clarity. Selected intramolecular distances (Å) in **1α**: Te1-Cl2 2.464(5), Te1-Cl1 2.468(4), Cl4-Te1 2.996(2); Selected intermolecular distances (Å) in **1α**: C5-Te1 3.722(6), C6-Te1 3.662(5), Cl4-C13 3.484(5); Selected intramolecular distances (Å) in **1β**: Te1-Cl1 2.441(2), Te1-Cl2 2.312(2), Te1-Cl4 2.984(2); Selected intermolecular distances (Å in **1β**: Te1-Cl3 3.450(2), C4-Cl4 3.485(7), C3–Cl4 3.433(7). All further attempts to recrystallize the crude product **1β** resulted in the formation of only **1α**.

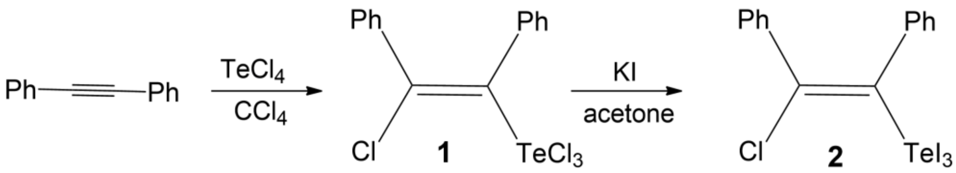

Figure 2. Preparation of Cl(Ph)C=C(Ph)$TeCl_3$ (**1**), and Cl(Ph)C=C(Ph)TeI_3 (**2**).

Crystallization of the CH_2Cl_2 extract of the reaction mixture afforded the isomorphic to the **1β** form of Cl(Ph)C=C(Ph)TeI_3 (**2β**, Figure 3a). Similar to **1β**, its recrystallization afforded **2α** crystals with a similar Te$\cdots$π(Ph) chain pattern. The latter is not exactly isomorphic to **1α**, but can be considered as a thermodynamic form of Cl(Ph)C=C(Ph)TeI_3 (Figure 3b, see Sections 3.3 and 3.4)

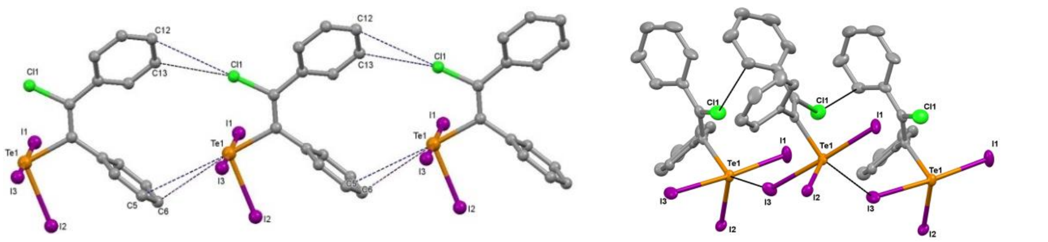

(**a**) (**b**)

Figure 3. Packing pattern of *Z*-Cl(Ph)C=C(Ph)TeI_3 molecules in the polymorphic forms **2α** (**a**) and **2β** (**b**). Hydrogen atoms are omitted for clarity. Selected intramolecular distances in **2α** (Å): Te1-I1 2.9918(4), Te1-I3 2.8530(4), Te1-I2 2.7395(8) Selected intermolecular distances in **2α** (Å): Te1-C6 3.630(5), Cl1-C13 3.533(7), C12-Cl1 3.617(7), Te1-Cl1 3.141(1) Selected intramolecular distances in **2β** (Å): Te1 I3 2.930(1), Te1 I1 2.885(1), Te1 I2 2.709(1) Selected intermolecular distances in **2β** (Å): I3 Te1 3.564(1), Cl1 C14 3.54(1), C9 Cl1 3.65(1), Selected angles (°): C1 Te1 I3 139.1(3), Te1 I3 Te1 135.54(3).

It is noteworthy that trichloride **1** reacts with acetone in a moderate yield of 54% only at reflux for 4 h [23] so that only known polymorphic form **1α** (BESHOW [16]) was recovered after the overnight stirring of **1β** solution in acetone at room temperature and no side reactions with acetone were noticed during the overnight stirring of powdered KI in **1β** solution in acetone (see Figure 2 and Section 2.1).

As a final remark on the molecular structure of **1–2**, we mention that Te atoms in these molecules seem to have pseudo-trigonal bipyramid (Ψ-TBP) surroundings, where the fifth position is occupied by intermolecular Te1$\cdots$π(Ph) (**α**) or Te1$\cdots$X3 (X = Cl (**1β**), I (**2α**) chalcogen bonds (see Figures 1 and 3). However, a closer look, motivated by our recent observations on Te geometry [9] drew attention to the possible intramolecular Te(1) $\cdots$ Cl(1) ChB (average distance ~3 Å), so that the sixth position is occupied or shielded by vinylic Cl atom and Te geometry in molecules **1–2** can be described as distorted octahedron, but not Ψ-TBP.

3.3. Supramolecular Organization Isomerism

Conformations of the isolated (Cl)PhC=CPh(TeX_3) molecules in the polymorphic pairs **1α** (*Pca*2_1)/**1β** (*Cc*) and **2α** (*P*2_1/*c*)/**2β** (*Cc*) are nearly identical (Figure 4), so we can consider them not as a case of conformational isomerism, but of supramolecular synthon isomerism [24,25].

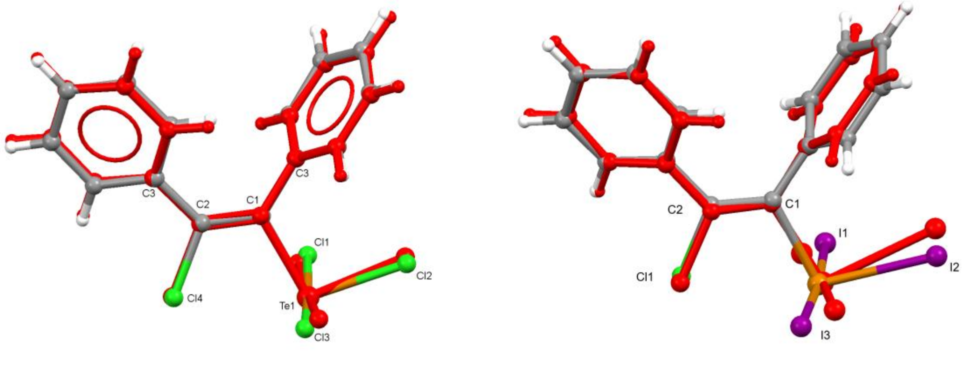

(**a**) (**b**)

Figure 4. Molecular structure overlay of (**a**) (Cl)PhC=CPh($TeCl_3$) molecules in **1α** (red) and **1β**; (**b**) (Cl)PhC=CPh(TeI_3) molecules in **2α** (red) and **2β**.

At the same time, crystals **1β** (*Cc*) and **2β** (*Cc*) are isomorphic, while **1α** (*Pca*2_1) and **2α** (*P*2_1/*c*) are not. Crystals **1α** and **2α** feature isostructural, [Te$\cdots\pi$Ph] stabilized chains (Figure 5), but these very isostructural chains are further packed differently relative to each other, following different angular geometry of type-I Cl$\cdots$Cl HaB and type-II I$\cdots$I HaBs (Figure 6).

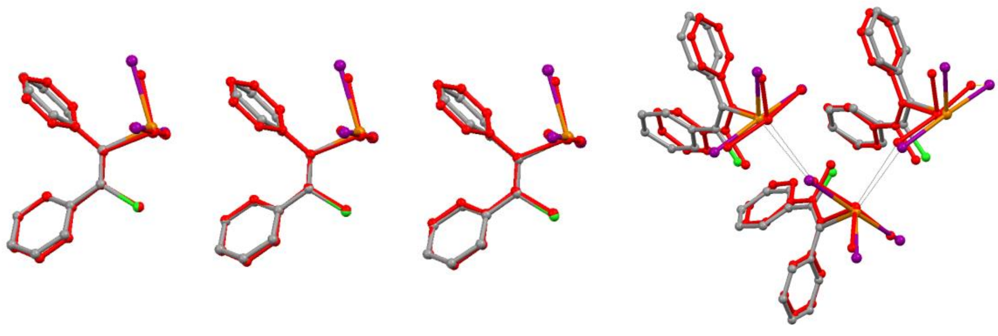

(**a**) (**b**)

Figure 5. Crystal structure overlay of (**a**) the straight-chain fragments in **1α** (red) and **2α**, and (**b**) overlay of zigzag chains in **1β** (red) and **2β**.

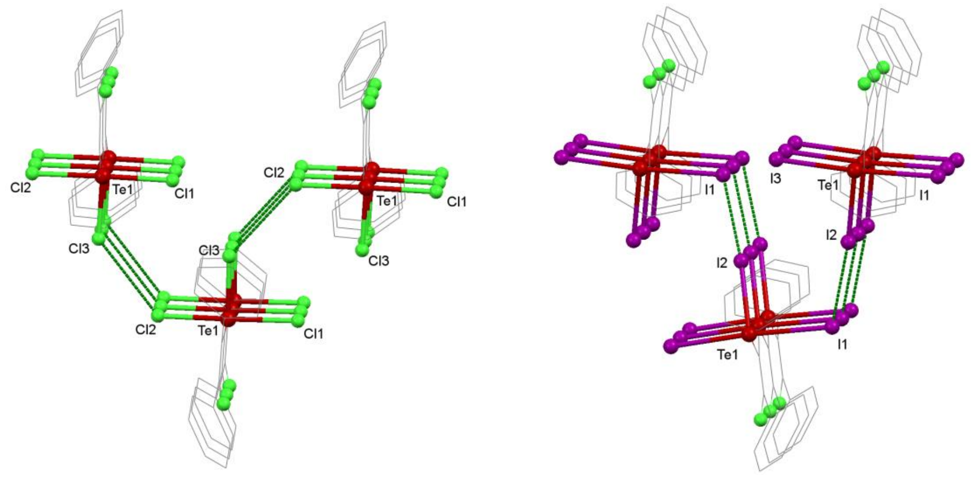

(**a**) (**b**)

Figure 6. Comparison of the mutual arrangement of chains in **1α** and **2α**. Notice different Te-Cl··· Cl and Te-I··· I angles corresponding to type-I and type-II HaBs, respectively: (**a**) Selected intermolecular angles (°): Te1-Cl2··· Cl3 127.94, Te1-Cl3··· Cl2 122.94; (**b**) Selected intermolecular angles (°): Te1-I2··· I1 174.53, Te1-I1··· I2 106.34. Selected intermolecular distances (Å): (**a**) Cl2-Cl3 3.719(7), (**b**) I2-I1 3.2852(8).

Although **1α** and **2α** are not isomorphic, the isostructural chain modules (Figure 5a) result in close values of the respective unit cell dimension (8.2010(8) and 8.2395(5)) with which they are parallel (Figure S1, Supplementary Materials). Further aggregation of these chain modules into the 3D structure is achieved by inter-chain Cl··· Cl and I··· I HaBs, but owing to the different tendencies of iodine and chlorine atoms for HaB, the arrangement of the chain modules is different in **1α** and **2α** (Figure 6). Easily polarized iodine atoms provide type-II I1··· I2 XBs in **2α** (Te1-I1··· I2 ~106° Te1-I2··· I1 ~174°, see Figure 6b), which direct the stretching of the respective unit cell dimension in **2α** (27.9101(17)Å) as compared to 21.031(3) Å in **1α**, where type-I Cl2··· Cl3 XBs does not have any notable structure-directing effect (Te1-Cl2··· Cl3~128°, Te1-Cl3··· Cl2~123°, Figure 6a).

The observation that crystals **1α** and **2α** are built of isostructural chains suggests that [Te··· πPh] may be a primary supramolecular synthon and therefore, these [Te··· πPh] chains themselves are the primary supramolecular synthon modules. Their further association is built upon the secondary [Cl··· Cl (type-I)] and [I··· I (type-II)] SSs, respectively, and owing to the difference between these secondary SSs, we can speak of the long-range synthon module isomerism in **1–2**. This is also an illustrative example of the 1D-to-2D stage of the Kitaigorodsky Aufbau Principle (KAP) [26–28], which anticipates the stepwise growth of dimensionality in the process of crystal formation.

3.4. Energy Frameworks of Ph(Cl)C=C(Ph)TeX$_3$ (X = Cl, I)

Certainly, short intermolecular contacts themselves do not imply a strong interaction [29] or a crystal structure-determining motif [30]. The functionality of Crystal Explorer software [21] favourably combines fast calculations of pairwise intermolecular interaction energies (B3LYP DGDZVP) and visualization of their magnitude in molecular clusters as Energy Frameworks [20]. This allows the construction of energetically based molecular packing patterns that may match, and thus support, patterns derived from evident short contacts or, conversely, can reveal overlooked or non-obvious supramolecular patterns [30]. Such calculation of the intermolecular interaction energy (B3LYP-DGDZVP TONTO/Crystal Explorer 21.5) in **1** and **2**, demonstrates that short Te··· Cl and Te··· C$_{Ph}$ contacts are observed in the pairs of molecules with the maximum binding energy (**1β**) or in the third-ranking (**1α**) in the top three of the strongest intermolecular interactions in the respective crystal (Figures 7a and 8b). Energy frameworks visualize these interactions as straight (**1α**) and zigzag (**1β**) chains (Figure 6.)

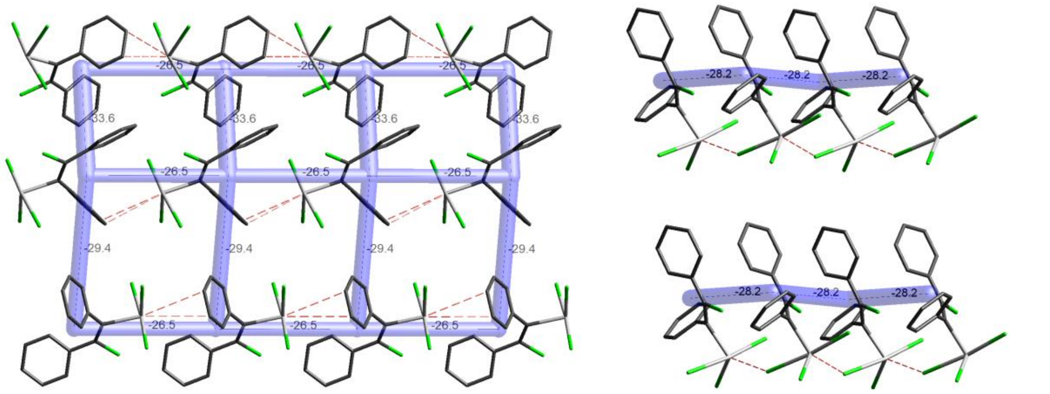

(**a**) (**b**)

Figure 7. (**a**) Straight line and (**b**) zigzag energy frameworks of **1α** and **1β,** respectively. Solid blue lines show total energy framework (Crystal Explorer 21.5, cut-off 22 kJ/mol). Intermolecular interaction energy values are indicated in kJ/mol.

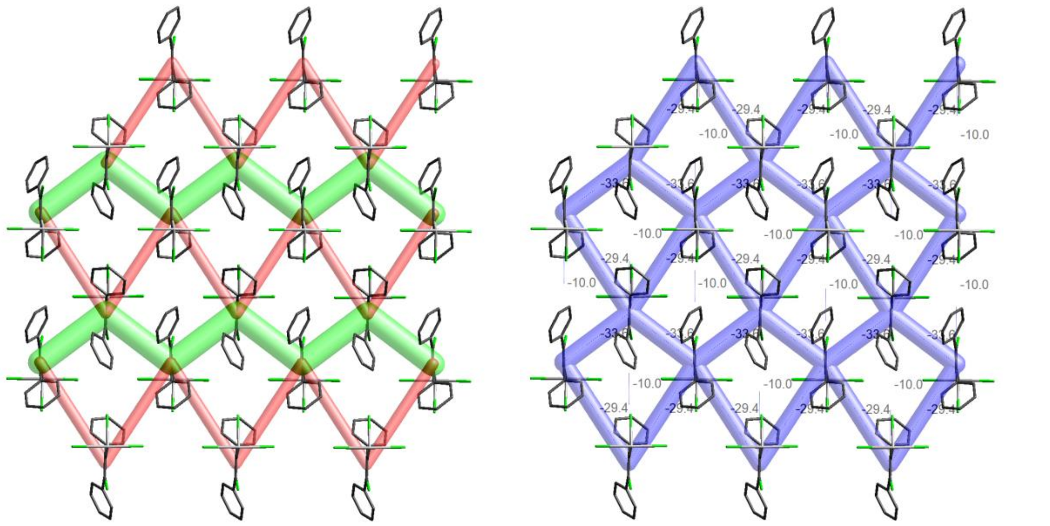

(**a**) (**b**)

Figure 8. Energy frameworks of **1α**, showing the contribution of dispersion and electrostatic interactions into the total intermolecular interaction energy (**a**) and total intermolecular interaction energy (**b**). Color code: red (electrostatic, cut-off 20 kJ/mol), green (dispersion, cut-off 25 kJ/mol). Blue cylinders show total energy framework (Crystal Explorer 21.5, cut-off 12 kJ/mol). Intermolecular interaction energy values are indicated in kJ/mol.

The orthogonal-to-chain direction cut of the energy framework of **1α** and **2α** (Figure 6) shows the interactions between the chains. built upon the secondary [Cl$\cdots$Cl (type-I)] and [I$\cdots$I (type-II)] supramolecular synthons, respectively. It also demonstrates that strong electrostatic interactions (mostly contributed by type-II I$\cdots$I HaBs) dominate over the dispersion interactions in **2α** (Figure 8).

Although the Te$\cdots$Cl pair in **1α** appears as the third-ranking interaction (−24,6 kJ/mol, Figures 7a and 8b, Table S2), it arises in the simple translation-related 1D chain. Such a fundamental symmetric relationship to the translation or screw axis is another powerful structure-determining factor [31]. Thus chemically meaningful and specific Te$\cdots$Cl and Te$\cdots\pi$Ph chalcogen bonds in **1–2** could be the structure determining interactions which provide the chemical recognition, which in turn governs the supramolecular association at the earliest, kinetic stages of crystal genesis. This suggests that structure-directing factors are defined not merely by the strongest intermolecular interactions, but by their combination with the symmetry operators resulting from the straightest chains (e.g., simple translation).

It should be mentioned that Te$\cdots$X and Te$\cdots\pi$Ph interactions in **1–2** are the strongest, but not outstanding, and are just 2–4 kJ/mol stronger than the second-ranking interactions (Tables S2–S5).

The resulting energy framework for **1**, **2**, built with a slightly lower cut-off (20 kJ/mol, Figure 9) presents a dense network of strong intermolecular interactions with no clear “weak links” where a second component can be inserted, providing a stronger lattice In contrast to the crystals, which have a significant gap between the chains or layers of the strongest interactions in their energy framework, so allowing the penetration of the guest molecules [32], we can assume that **1–2** are poor conformers for the design of co-crystals stabilized by X$\cdots$A XBs or Te$\cdots$X ChBs with the second ChB/XB-donor or acceptor component. Indeed, an attempted co-crystallization of **1** and **2** with the iconic HaB-donor (1,4-diiodo tetrafluorobenzene) and HaB-acceptor (pyridine) showed their low affinity for the formation of the ChB/HaB-stabilized two-component crystals.

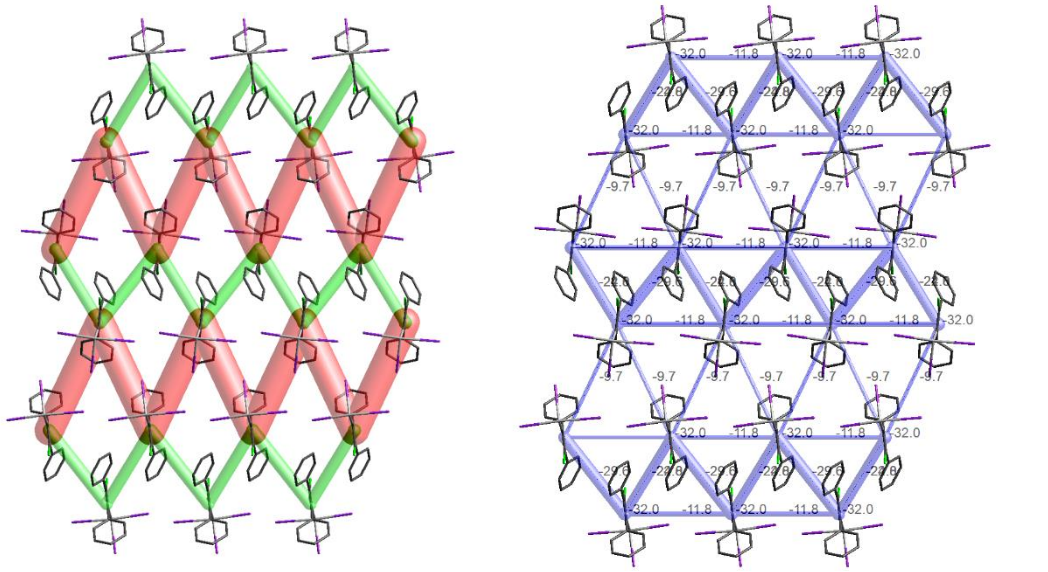

Figure 9. Energy frameworks of **2α**, showing the contribution of dispersion and electrostatic interactions into the total intermolecular interaction energy (**a**) and total intermolecular interaction energy (**b**). Color code: red (electrostatic, cut-off 20 kJ/mol), green (dispersion, cut-off 28 kJ/mol). Blue cylinders show total energy framework (Crystal Explorer 21.5, cut-off 9 kJ/mol). Intermolecular interaction energy values are indicated in kJ/mol.

Intermolecular energy calculations (TONTO CE-B3LYP/DGDZVP) demonstrated the ~1 kcal/mol difference in the lattice stabilization energies in **1α/1β** and **2α/2β** pairs (see Table S1). Such a difference is typical for the polymorphs’ and is supported by preliminary (based on their crystallization conditions) assignment of **α** and **β** as thermodynamic and kinetic forms, respectively.

Although the triiodide polymorphs **2α** and **2β** can be prepared by varying the crystallization conditions, **1β** looks elusive, not to say, disappearing polymorph [33,34].

4. Conclusions

In this work, two new polymorphic pairs of $Ph_2C_2(Cl)TeI_3$ (**1α** and **1β**) and $Ph_2C_2(Cl)TeI_3$ (**2α** and **2β**) were structurally characterized. Although their presumably kinetic forms (**1α** and **2α**) are isostructural and isomorphic, the structures of the respective thermodynamic forms (**1β** and **2β**) demonstrate only partial similarity. They reveal isostructural primary chain-like modules which are subsequently packed differently following the different geometry and energetics of intermolecular I···I and Cl···Cl HaBs. This phenomenon can be defined as long-range aufbau supramolecular synthon modules isomerism.

Supplementary Materials: The following supporting information can be downloaded at https://www.mdpi.com/article/10.3390/chemistry4010017/s1. Figure S1: Fragments of the packing in (a) 1α Pca21 a 21.031(3) b 8.2010(8) c 9.215(1) and (b) 2α P21/c a 8.2395(5) b 27.9101(17) c 8.7289(5)s; Figure S2: Theoretical powder diffraction patterns of 1α-polymorph (black) and 1β-polymorph (red) and experimental patterns of the crystalline sample 1β (blue); Figure S3: Final fit of the Rietveld refinement of the structure 1β (Rwp = 0.031): experimental X-ray diffraction pattern (black), Pawley fit (red) and difference profile (gray); Figure S4: Theoretical powder diffraction patterns of 1α-polymorph (black) and 1β-polymorph (red) and experimental patterns of the crystalline sample 1α (green); Figure S5: Final fit of the Rietveld refinement of the structure 1α (Rwp = 0.067): experimental X-ray diffraction pattern (black), Pawley fit (red) and difference profile (gray); Figure S6: Theoretical powder diffraction patterns of 2α-polymorph (brown) and 2β-polymorph (blue) and experimental patterns of the crystalline sample 2β (magenta); Table S1. Lattice energy Calculated in Crystal Explorer 17.5 (CE-B3LYP-DGDZVP, 25 Å cluster); Table S2. Interaction Energies (kJ/mol) in 1α; Table S3. Interaction Energies (kJ/mol) in 1β; Table S4. Interaction Energies (kJ/mol) in 3α; Table S5. Interaction Energies (kJ/mol) in 3β.

Author Contributions: Conceptualization, experiment, original draft preparation, Y.V.T.; XRD analysis, manuscript editing, A.S.S. All authors have read and agreed to the published version of the manuscript.

Funding: This research was funded by the Ministry of Science and Higher Education of the Russian Federation as part of the State Assignment of the Kurnakov Institute of General and Inorganic Chemistry of the Russian Academy of Sciences.

Data Availability Statement: Atomic coordinates and other structural parameters of 1-x have been deposited with the Cambridge Crystallographic Data Centre: CCDC 2125950 (1β), CCDC 2125951 (2α) and CCDC 2125949 (2β).

Acknowledgments: We thank F. M. Dolgushin (IGIC RAS) for valuable discussion.

Conflicts of Interest: The authors declare no conflict of interest. The funders had no role in the design of the study; in the collection, analyses, or interpretation of data; in the writing of the manuscript; or in the decision to publish the results.

References

1. Sonnenberg, K.; Mann, L.; Redeker, F.A.; Schmidt, B.; Riedel, S. Polyhalogen and Polyinterhalogen Anions from Fluorine to Iodine. *Angew. Chem. Int. Ed. Engl.* **2020**, *59*, 5464–5493. [CrossRef]
2. Vogel, L.; Wonner, P.; Huber, S.M. Chalcogen Bonding: An Overview. *Angew. Chem. Int. Ed.* **2019**, *58*, 1880–1891. [CrossRef] [PubMed]
3. Tiekink, E.R.T. Supramolecular assembly based on "emerging" intermolecular interactions of particular interest to coordination chemists. *Coord. Chem. Rev.* **2017**, *345*, 209–228. [CrossRef]
4. Bulfield, D.; Engelage, E.; Mancheski, L.; Stoesser, J.; Huber, S.M. Crystal Engineering with Multipoint Halogen Bonding: Double Two-Point Donors and Acceptors at Work. *Chemistry* **2020**, *26*, 1567–1575. [CrossRef] [PubMed]
5. Biot, N.; Bonifazi, D. Concurring Chalcogen- and Halogen-Bonding Interactions in Supramolecular Polymers for Crystal Engineering Applications. *Chemistry* **2020**, *26*, 2904–2913. [CrossRef] [PubMed]
6. Eichstaedt, K.; Wasilewska, A.; Wicher, B.; Gdaniec, M.; Połoński, T. Supramolecular Synthesis Based on a Combination of Se···N Secondary Bonding Interactions with Hydrogen and Halogen Bonds. *Cryst. Growth Des.* **2016**, *16*, 1282–1293. [CrossRef]
7. Li, B.; Zang, S.-Q.; Wang, L.-Y.; Mak, T.C.W. Halogen bonding: A powerful, emerging tool for constructing high-dimensional metal-containing supramolecular networks. *Coord. Chem. Rev.* **2016**, *308*, 1–21. [CrossRef]
8. Aakeroy, C.B.; Baldrighi, M.; Desper, J.; Metrangolo, P.; Resnati, G. Supramolecular hierarchy among halogen-bond donors. *Chemistry* **2013**, *19*, 16240–16247. [CrossRef]
9. Torubaev, Y.V.; Dolgushin, F.M.; Skabitsky, I.V.; Popova, A.E. Isomorphic substitution in molecular crystals and geometry of hypervalent tellurium: Comments inspired by a case study of $RMeTeI_2$ and $[RMe_2Te]^+I^-$ (R. = Ph, Fc). *New J. Chem.* **2019**, *43*, 12225–12232. [CrossRef]
10. Chivers, T.; Laitinen, R.S. Tellurium: A maverick among the chalcogens. *Chem. Soc. Rev.* **2015**, *44*, 1725–1739. [CrossRef] [PubMed]

11. Zukerman-Schpector, J.; Haiduc, I. Tellurium···π-aryl interactions: A new bonding motif for supramolecular self-assembly and crystal engineering. *CrystEngComm* **2002**, *4*, 178–193. [CrossRef]
12. Wang, W.; Ji, B.; Zhang, Y. Chalcogen Bond: A Sister Noncovalent Bond to Halogen Bond. *J. Phys. Chem. A* **2009**, *113*, 8132–8135. [CrossRef] [PubMed]
13. Torubaev, Y.; Pasynskii, A.; Mathur, P. Organotellurium halides: New ligands for transition metal complexes. *Coord. Chem. Rev.* **2012**, *256*, 709–721. [CrossRef]
14. Torubaev, Y.V.; Lyssenko, K.A.; Popova, A.E. Halogen and Hydrogen Bonds in Co-crystalline Ferrocenium Organotellurium Halide Salts. *Russ. J. Coord. Chem.* **2019**, *45*, 788–794. [CrossRef]
15. Petragnani, N.; Mendes, S.R.; Silveira, C.C. Tellurium tetrachloride: An improved method of preparation. *Tetrahedron Lett.* **2008**, *49*, 2371–2372. [CrossRef]
16. Zukerman-Schpector, J.; Camillo, R.L.; Comasseto, J.V.; Santos, R.A.; Caracelli, I. Trichloro[(Z)-2-chloro-1,2-diphenylvinyl]tellurium(IV). *Acta Crystallogr. Sect. C* **1999**, *55*, 1577–1579. [CrossRef]
17. Dolomanov, O.V.; Bourhis, L.J.; Gildea, R.J.; Howard, J.A.K.; Puschmann, H. OLEX2: A complete structure solution, refinement and analysis program. *J. Appl. Cryst.* **2009**, *42*, 339–341. [CrossRef]
18. Sheldrick, G.M. Crystal structure refinement with SHELXL. *Acta Crystallogr. Sect. C Struct. Chem.* **2015**, *71*, 3–8. [CrossRef]
19. Coelho, A.A. TOPASandTOPAS-Academic: An optimization program integrating computer algebra and crystallographic objects written in C++. *J. Appl. Crystallogr.* **2018**, *51*, 210–218. [CrossRef]
20. Mackenzie, C.F.; Spackman, P.R.; Jayatilaka, D.; Spackman, M.A. CrystalExplorer model energies and energy frameworks: Extension to metal coordination compounds, organic salts, solvates and open-shell systems. *IUCrJ* **2017**, *4*, 575–587. [CrossRef]
21. Spackman, P.R.; Turner, M.J.; McKinnon, J.J.; Wolff, S.K.; Grimwood, D.J.; Jayatilaka, D.; Spackman, M.A. CrystalExplorer: A program for Hirshfeld surface analysis, visualization and quantitative analysis of molecular crystals. *J. Appl. Crystallogr.* **2021**, *54*, 1006–1011. [CrossRef] [PubMed]
22. Thomas, S.P.; Spackman, P.R.; Jayatilaka, D.; Spackman, M.A. Accurate Lattice Energies for Molecular Crystals from Experimental Crystal Structures. *J. Chem. Theory Comput.* **2018**, *14*, 1614–1623. [CrossRef] [PubMed]
23. Cunha, R.L.O.R.; Zukerman-Schpector, J.; Caracelli, I.; Comasseto, J.V. Revisiting the addition reaction of TeCl4 to alkynes: The crystal structure and docking studies of 1-chloro-2-trichlorotelluro-3-phenyl-propen-2-ol. *J. Organomet. Chem.* **2006**, *691*, 4807–4815. [CrossRef]
24. Aitipamula, S.; Chow, P.S.; Tan, R.B.H. Polymorphism in cocrystals: A review and assessment of its significance. *CrystEngComm* **2014**, *16*, 3451–3465. [CrossRef]
25. Torubaev, Y.V.; Skabitsky, I.V.; Anisimov, A.A.; Ananyev, I.V. Long-range supramolecular synthon polymorphism: A case study of two new polymorphic cocrystals of Ph2Te2–1,4-C6F4I2. *CrystEngComm* **2022**, *24*, 1442–1452. [CrossRef]
26. Kitaigorodskii, A.I. *Organic Chemistry Crytallography*; Consultants Bureau: New York, NY, USA, 1961.
27. Perlstein, J. Molecular Self-Assemblies. 4. Using Kitaigorodskii's Aufbau Principle for Quantitatively Predicting the Packing Geometry of Semiflexible Organic Molecules in Translation Monolayer Aggregates. *J. Am. Chem. Soc.* **2002**, *116*, 11420–11432. [CrossRef]
28. Torubaev, Y.; Skabitsky, I.; Lyssenko, K.A. Stages of Kitaigorodsky Aufbau Principle Detached in the Cocrystals of Cp_2MX_2 (M = Ti, Zr; X = Cl, Br, I) with σ- and π-Hole Donors. *Cryst. Growth Des.* **2022**, *22*, 1244–1252. [CrossRef]
29. Dunitz, J.D. Intermolecular atom-atom bonds in crystals? *IUCrJ* **2015**, *2*, 157–158. [CrossRef] [PubMed]
30. Torubaev, Y.V.; Skabitsky, I.V.; Saratov, G.A.; Barzilovich, P.Y. Halogen vs. ionic bonding: An unusual isomorphism between the neutral $(C_5Me_5)_2Fe/C_2I_2$ cocrystal and ionic $[(C_5Me_5)_2Fe]Br_3$ crystal. *Mendeleev Commun.* **2021**, *31*, 58–61. [CrossRef]
31. Gavezzotti, A. Pillars of crystal engineering: Crystal energies and symmetry operators. *CrystEngComm* **2018**, *20*, 2511–2518. [CrossRef]
32. Torubaev, Y.V.; Rai, D.K.; Skabitsky, I.V.; Pakhira, S.; Dmitrienko, A. Energy framework approach to the supramolecular reactions: Interplay of the secondary bonding interaction in Ph_2E_2 (E = Se, Te)/*p*-I-$C_6F_4I_2$ co-crystals. *New J. Chem.* **2019**, *43*, 7941–7949. [CrossRef]
33. Dunitz, J.D.; Bernstein, J. Disappearing Polymorphs. *Acc. Chem. Res.* **2002**, *28*, 193–200. [CrossRef]
34. Bucar, D.K.; Lancaster, R.W.; Bernstein, J. Disappearing polymorphs revisited. *Angew. Chem. Int. Ed. Engl.* **2015**, *54*, 6972–6993. [CrossRef] [PubMed]